

Chapter 9

Statistical Analysis of Absorbers

9.1 Surveys

In surveys, one is often interested in obtaining an objective census of all the absorption lines in the spectrum. This usually consists of a “line list” comprising central wavelengths, equivalent widths, uncertainties in the equivalent widths, and significance levels of the features. Normally, low to intermediate resolution spectra, those with $R < 5000$, are employed for surveys.

Surveys of absorption lines usually focus on one class of system, such as $\text{Ly}\alpha$ forest clouds, Lyman limit systems (LLS), Damped $\text{Ly}\alpha$ absorbers (DLAs), or metal line systems such as Mg II , C IV , or O VI absorbers. Scientific objectives often include constraining the fiducial size (absorption cross-sections), number density, equivalent width distribution, redshift clustering, metallicities, and mean mass densities (in terms of the closure density) of absorbing gas. Another common objective is to constrain the intensity and spectral energy distribution of the global ultraviolet background radiation. However, this latter objective requires ionization modeling and will be addressed in later chapters.

A sample of quasars is almost always selected based upon practical issues such as observing window (time of year), quasar brightness, detection sensitivity limit, desired statistical significance of scientific results, etc. It is assumed that all lines of sight are statistically independent. Exceptions to this rule are surveys that aim to establish the correlation lengths of the absorbers using quasars with small angular separations. These multiple line of sight observations will be treated in later chapters.

In Figure 9.1, a schematic of a quasar absorption line survey is illustrated. The observer is located at the center (left panel) and measures the redshifts of various absorbers (filled dots) along the lines of sight (radial lines) toward different quasars having different redshift at different locations in the sky. In the case that the lines of sight are independent, the counting of absorbers can be collapsed onto a single redshift line.

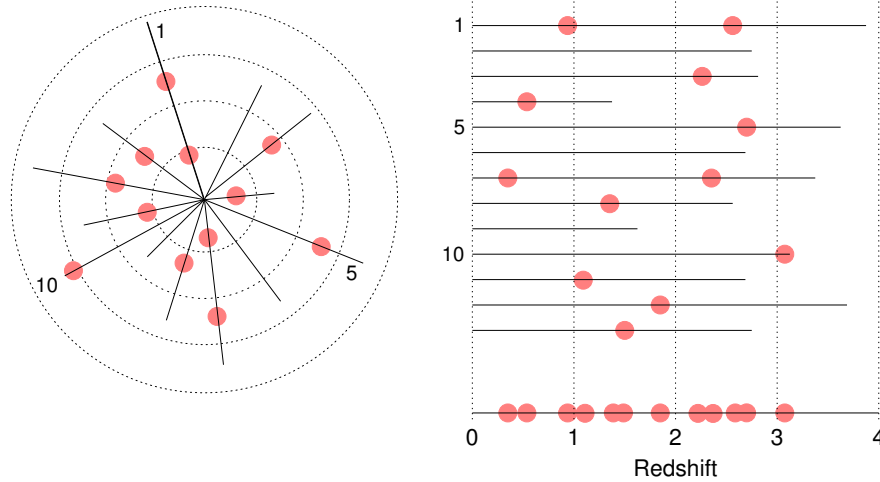


Figure 9.1: — A schematic of a typical quasar absorption line survey. — (left) The quasars are randomly distributed in space and are at different redshifts. The dotted concentric circles represent redshifts $z = 1, 2, 3$, and 4 , respectively, with respect to the observer at the origin. Intervening absorbers (shaded points) at various redshifts will be intercepted along most quasar lines of sight. — (right) The absorbers observed along each independent line of sight can be “collapsed” into a single line of sight (bottom solid line) as long as the *total* redshift path covered by the ensemble of quasars is properly accounted. The accounting is quantified using the redshift path sensitivity function, Eq. 9.4.

However, to deduce evolution (or lack of) in an absorber population, it is critical to make a proper and detailed accounting of the survey selection effects. These selection effects include both the sensitivity limitations of the survey, which may be a function of redshift, and the unique nature of pencil beam surveys. The former is usually treated by computing a so-called redshift path sensitivity function, whereas the inclusion of the behavior of the pencil beam survey methodology requires accounting for the probability of intersecting extended objects along the line of sight to quasars.

9.2 Redshift Path Sensitivity Function

For each quasar, there is a redshift path that, in principle, can range from $z_{min} = 0$ to $z_{max} = z_{em}$, where z_{em} is the redshift of the quasar determined from its emission lines. In practice, the redshift path is governed by the observed wavelength range, which is instrument dependent, and the rest-frame wavelength λ_r of the transition representing the type of system being surveyed. If the observed wavelength range of a quasar is λ_{min} to λ_{max} , then the redshift path for the quasar is

$$\Delta Z = z_{max} - z_{min} \quad (9.1)$$

where

$$z_{min} = \begin{cases} 0 & : \lambda_r \geq \lambda_{min} \\ \lambda_{min}/\lambda_r - 1 & : \lambda_r < \lambda_{min}, \end{cases} \quad (9.2)$$

and

$$z_{max} = \begin{cases} z_{em} & : \lambda_r(1 + z_{em}) < \lambda_{max} \\ \lambda_{max}/\lambda_r - 1 & : \lambda_r(1 + z_{em}) \geq \lambda_{max}. \end{cases} \quad (9.3)$$

Consider a sample of M quasars, where the k th quasar has a redshift path ranging from z_k^{min} to z_k^{max} . Then the redshift path sensitivity function is

$$g(z) = \sum_{k=1}^M H(z - z_k^{min})H(z_k^{max} - z) \quad (9.4)$$

summed over all quasars, where

$$z = \frac{\lambda}{\lambda_r} - 1 \quad (9.5)$$

is the redshift, and where $H(t)$ is the Heavisite step function with

$$H(t) = \begin{cases} 0 & : t < 0 \\ 1 & : t \geq 0. \end{cases} \quad (9.6)$$

The values of $g(z)$ are integers giving the number of quasars in which the target system could have been observed at redshift z .

In practice, a grid stepped in intervals $\delta z = \Delta\lambda_{pix}/\lambda_r$, where $\Delta\lambda_{pix}$ is the wavelength interval of a pixel at wavelength λ . The range of the z grid is taken to be the minimum and maximum redshifts of the quasars in the sample. Then, $g(z)$ is computed at each z location in the grid. The run of $g(z)$ versus z provides the redshift path sensitivity of the survey. The total redshift path for the survey is then

$$\Delta Z = \int_0^\infty g(z)dz, \quad (9.7)$$

which can be computed more simply from

$$\Delta Z = \sum_{k=1}^M (z_k^{max} - z_k^{min}) \quad (9.8)$$

However, as written, Eqs. 9.4 and 9.8 do not account for the fact that the detection sensitivity is not uniform at all redshifts along the path. Usually, the sensitivity is defined as an arbitrary rest-frame equivalent width detection threshold, denoted W_{min} . As discussed in § 8.1.1, the observed equivalent width detection threshold in a pixel is given by σ_{w_j} (Eq. 8.2 or 8.16). Then, at each redshift, the rest-frame equivalent width detection threshold at λ is

$$w_{min}(z) = \frac{\sigma_w(\lambda)}{1+z} = \frac{\sigma_w(\lambda)}{(\lambda/\lambda_r)} \quad (9.9)$$

Generalizing Eq. 9.4, we have the number of quasars (or lines of sight) at which a target absorption line with rest-frame equivalent width W_{min} or greater could be detected at a significance level of N_σ at redshift z ,

$$g(W_{min}, z) = \sum_{k=1}^M H(z - z_k^{min}) H(z_k^{max} - z) H(w_{min}(z) - N_\sigma W_{min}). \quad (9.10)$$

The total redshift path for a detection threshold W_{min} is then

$$\Delta Z(W_{min}) = \int_0^\infty g(W_{min}, z) dz. \quad (9.11)$$

In practice, $g(W_{min}, z)$ for a survey is computed as a discretized grid in δW_{min} and δz appropriate to the survey goals, distribution of signal-to-noise ratios of the spectra, spectral coverage, and pixelization of the spectra. Then the total redshift path is computed for each W_{min} by summing the grid in the z direction

$$\Delta Z(W_{min}) = \sum g(W_{min}, z) \delta z. \quad (9.12)$$

9.3 Redshift Number Density

The redshift number density is the number of absorbers per unit redshift. As we shall see in § 9.4, it constrains the product of the number density and cross section of the absorbers. It is desirable that the survey is unbiased to the detection sensitivity of the absorption strength *and* the sample of quasars is selected with no *a priori* knowledge of absorbers toward the

quasars. To enforce the former criterion, a minimum equivalent width is selected for all redshifts. This detection threshold is driven by the sensitivity, or signal-to-noise ratio, of the spectra.

If N_{abs} absorbers with $W_r \geq W_{min}$ are detected in a survey with redshift path $\Delta Z(W_{min})$, then the number of absorbers per unit redshift, denoted $\mathcal{N}(z)$ and often written as dN/dz , is

$$\mathcal{N}(\langle z \rangle) \equiv \frac{dN(\langle z \rangle)}{dz} = \frac{N_{abs}}{\Delta Z(W_{min})}, \quad (9.13)$$

where $\langle z \rangle$ simply indicates that the value of $\mathcal{N}(z)$ applies for the median redshift of the observed systems with $W_r \geq W_{min}$ over the redshift path. The uncertainty in $\mathcal{N}(z)$ is obtained by proper Poisson statistics, which in the case of N_{abs} approaches greater than 10, becomes

$$\sigma_{\mathcal{N}} = \frac{\sqrt{N_{abs}}}{\Delta Z(W_{min})} \quad (9.14)$$

It is common to bin the redshift intervals in order to compare the redshift behavior of $\mathcal{N}(z)$. The proper redshift path must be computed for each bin. If $N_{abs,i}$ absorbers with $W_r \geq W_{min}$ are detected in the i th redshift bin, then

$$\mathcal{N}_i(\langle z_i \rangle) = \frac{N_{abs,i}}{\Delta Z_i(W_{min})}, \quad (9.15)$$

where, $\langle z_i \rangle$ is the median redshift of the detected absorbers with $W_r \geq W_{min}$ between the lower and upper redshift limits, z_i^{min} and z_i^{max} , of the bin

$$\Delta Z_i(W_{min}) = \sum g(W_{min}, z) \delta z \quad \text{for } z_i^{min} \leq z < z_i^{max}, \quad (9.16)$$

where δz is the $g(W_{min}, z)$ grid resolution. Note that one edge of the bin is inclusive and the other is exclusive. As can be seen from the above formalism, one can also examine $\mathcal{N}(z)$ for different W_{min} thresholds.

Consider the example survey shown in Figure 9.1. Assume spectral coverage of 3100–9000 Å and that C IV $\lambda\lambda 1548, 1550$ absorbers are being surveyed. Then $z_{min} = 3100/1548 - 1 = 1.0$, below which the C IV absorption lines are too blue to be captured in the spectra. The redshift sensitivity function, $g(z)$, is presented in Figure 9.2 (left panel) for the mock C IV survey assuming $W_{min} = 0$ and $\delta z = 0.1$ for the computation of $g(z)$ grid. In the right panel of Figure 9.2, the redshift number density of C IV absorbers is presented in 0.5 redshift bins, as computed using Eq. 9.15. No errors are included for this example.

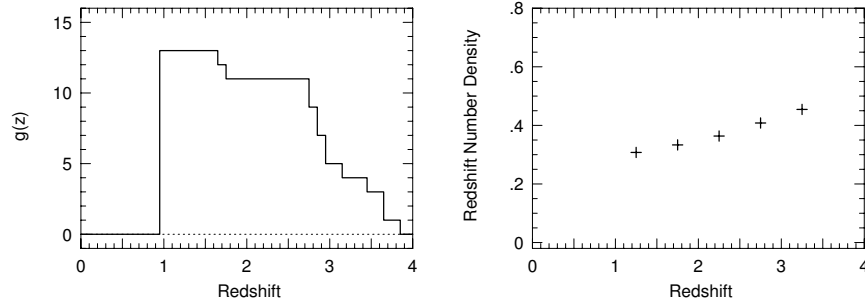


Figure 9.2: — (left) The redshift sensitivity function $g(z)$ from Eq. 9.4 for the mock survey of CIV absorbers shown in Figure 9.1 assuming all spectra have wavelength coverage 3100–9000 Å. — (right) The redshift path density computed from Eq. 9.15 for the mock CIV survey computed in redshift bins of 0.5. See text for additional explanation.

If the data are not suitable for forming an unbiased survey defined by W_{min} , then the accounting must allow for different line strengths to be detected over different redshifts. One calculates the redshift path over which each detected system could be found and computes the redshift density from

$$\mathcal{N}(z) = \sum_{j=1}^{N_{abs}} \frac{1}{\Delta Z(W_j)}, \quad (9.17)$$

where the sum is over the detected systems. The uncertainty is given by

$$\sigma_{\mathcal{N}}^2 = \sum_{j=1}^{N_{abs}} \frac{1}{\Delta Z^2(W_j)}. \quad (9.18)$$

This technique effectively weights the redshift path for each absorber's equivalent width as if it were the minimum equivalent width of the survey.

9.3.1 Redshift Density Evolution

The redshift density, $\mathcal{N}(z)$ is dependent upon the cosmological model and describes the number of objects intercepted in a co-moving path length. From the differential probability of intercepting an absorber long a line of sight in interval $z \rightarrow z + dz$ (Eq. 2.181), we have

$$\mathcal{N}(z) \equiv \frac{dN}{dz} = \frac{c}{H_o} n(z) \sigma(z) \frac{dX}{dz}, \quad (9.19)$$

where $n(z)$ is the number density of absorbers, $\sigma(z)$ is the absorber geometric cross section, and where dX/dz is the differential absorption distance defined in Eq. 2.177. Substituting Eq. 2.177, where $E(z)$ is given by Eq. 2.80, into Eq. 9.19 gives

$$\frac{dN}{dz} = N(z) \frac{(1+z)^2}{\sqrt{\Omega_m(1+z)^3 + \Omega_\Lambda}}, \quad (9.20)$$

where

$$N(z) = \frac{c}{H_o} n(z) \sigma(z). \quad (9.21)$$

The values of the densities for the currently fashionable concordance cosmological model are $\Omega_m \simeq 0.3$, and $\Omega_\Lambda \simeq 0.7$.

For a constant $N(z)$, we see that dN/dz increases monotonically with increasing redshift, as it should since it is describing the number of objects along an observed co-moving path length. In the absence of direct knowledge (or some pretty sound assumptions) of $n(z)$ and $\sigma(z)$, it is only $N(z)$ that can be constrained by the measured $\mathcal{N}(z)$. Assuming

$$N(z) = \frac{c}{H_o} n_o \sigma_o (1+z)^\varepsilon \quad (9.22)$$

to parameterize evolution, the redshift path density can be used to constrain evolution in $n(z)\sigma(z)$, giving

$$\frac{dN}{dz} = N_o \frac{(1+z)^{2+\varepsilon}}{\sqrt{\Omega_m(1+z)^3 + \Omega_\Lambda}}, \quad (9.23)$$

where the expression is evaluated for $z = \langle z \rangle$ of the absorber distribution, $N_o = (c/H_o)n_o\sigma_o$, and ε is the evolution parameter. The maximum likelihood method can then be employed to determine N_o and ε , and their uncertainties. For ε values inconsistent with zero, some form of evolution can be inferred for the product $n(z)\sigma(z)$.

From the definition of $\mathcal{N}(z)$ in Eq. 9.19, substitution of the differential absorption distance, dX/dz , for a Friedmann cosmology (Eq. 2.179), yields

$$\frac{dN}{dz} = N(z) \frac{(1+z)}{\sqrt{1+2q_o z}}, \quad (9.24)$$

where, as before, $N(z) = n(z)\sigma(z)$. Analogous to Eq. 9.22, it is useful to parameterize redshift number density evolution using, yielding

$$\frac{dN}{dz} = N_o (1+z)^\gamma, \quad (9.25)$$

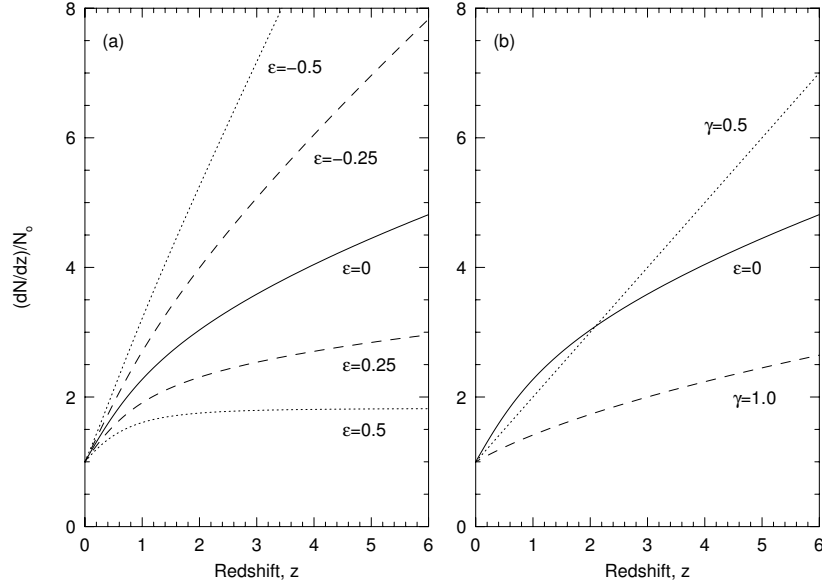


Figure 9.3: — (a) The redshift path density, normalized to N_o for a concordance model ($\Omega_m = 0.3$, $\Omega_\Lambda = 0.7$) for evolution parameters $\epsilon = -0.5, -0.25, 0, +0.25$, and $+0.5$. — (b) The redshift path density, normalized to N_o for the Friedmann model for evolution parameters $\gamma = 0.5$ and 1.0 , corresponding to $q_o = 1/2$ and $q_o = 0$, respectively. The no-evolution curve of the concordance model is shown for comparison.

where the evolution parameter, γ , is used to denote the Friedmann cosmology and ranges between 0.5–1.0 depending upon the value of q_o ,

$$\gamma = \begin{cases} 1 & : q_o = 0 \\ & : \\ 1/2 & : q_o = 1/2. \end{cases} \quad (9.26)$$

In Figure 9.3, dN/dz is shown for various evolution parameters. In panel *a*, the concordance model is shown and in panel *b* the Friedmann model is compared to the no-evolution curve of the concordance model. Virtually all quasar absorption line work in the literature prior to 2000 used Eq. 9.25 to parameterize absorber evolution. This form is still used, but more often the expression for concordance model is being used, not only for $\mathcal{N}(z)$, but for all statistical quantities in quasar absorption line surveys.

9.3.2 Absorption Distance Density

The absorption distance density, $\mathcal{N}(X)$, illustrates an interesting point and can provide a more direct measurement for evolution. The redshift density, $\mathcal{N}(z)$ in a redshift interval $z \rightarrow z + dz$ is related to the absorption distance density in a absorption distance interval $X \rightarrow X + dX$ by

$$\mathcal{N}(z)dz = \mathcal{N}(X)dX, \quad (9.27)$$

which gives the relationship

$$\mathcal{N}(X) = \mathcal{N}(z) \frac{dz}{dX}, \quad (9.28)$$

Substituting Eq. 9.28 into Eq. 9.19, and invoking $dz/dX = (dX/dz)^{-1}$, we have

$$\mathcal{N}(X) = \frac{c}{H_o} n(X) \sigma(X), \quad (9.29)$$

where $n(X)$ is the absorber number density, $\sigma(z) = \sigma(X)$ is uncoupled to the cosmology. For a non-evolving population of absorbers fixed in co-moving coordinates, the redshift distance density is a constant. Thus, a statistically significant departure of $\mathcal{N}(X)$ from a constant provides a direct measured of evolution in the product $n(X)\sigma(X)$.

The computation of $\mathcal{N}(X)$ is analogous to the computation of $\mathcal{N}(z)$ except that one needs to compute the sensitivity function for the absorption distance of the survey. The absorption distance, $X(z)$, is given by Eq. 2.178,

$$X(z) = \int_0^z \frac{(1+z)^2}{E(z)} dz, \quad (9.30)$$

and by Eq. 2.180 for a Friedmann cosmology. Computing the absorption distance sensitivity is fully analogous to computing the redshift path sensitivity. It is computed using

$$g(W_{min}, X) = \sum_{k=1}^M H(X - X_k^{min}) H(X_k^{max} - X) H(w_{min}(X) - N_\sigma W_{min}), \quad (9.31)$$

where the terms have the same meaning as in Eq. 9.10. As with the $g(z)$, the $g(X)$ are integers giving the number of quasars in which the target system could have been observed at $X(z)$. In practice, the range of X is taken as the minimum X^{min} and the maximum X^{max} of the quasars in the sample and X is computed on a grid of small intervals on the order of $\delta x = (dX/dz)(\Delta\lambda_{pix}/\lambda_r)$, where the latter term is δz in terms of the

redshift interval of a typical pixel, and dX/dz is obtained from Eq. 2.177

$$\frac{dX}{dz} = \frac{(1+z)^2}{E(z)}, \quad (9.32)$$

or by Eq. 2.179 for a Friedmann cosmology. . The total absorption distance for the survey is then computed from the $g(W_{min}, X)$ grid using

$$\Delta X(W_{min}) = \sum g(W_{min}, X) \delta x. \quad (9.33)$$

Again, it is common to bin redshift distance intervals in order to examine evolution in $\mathcal{N}(z)$. We have,

$$\mathcal{N}_i(\langle z_i \rangle) = \frac{N_{abs,i}}{\Delta X_i(W_{min})}, \quad (9.34)$$

where

$$\Delta X_i(W_{min}) = \sum g(W_{min}, z) \delta x \quad \text{for} \quad X_i^{min} \leq z < X_i^{max}, \quad (9.35)$$

where, $\langle z_i \rangle$ is the median redshift of the detected absorbers with $W_r \geq W_{min}$ between the lower and upper limits of the i th bin.

9.4 Sizes of Absorbers

The absorbers cross sections can be estimated if assumptions about the number density, $n(z)$, and cross section, $\sigma(z)$, are made. The most common assumption is that the gas is associated with galaxies. Under this assumption, we can equate $n(z)$ with the number density of galaxies, which is obtained by integrating the galaxy luminosity function (expressed as a number per unit volume per unit luminosity) over all luminosities. To obtain $N(z)$, the luminosity function needs to be weighted by the cross sections, or sizes, of the absorbing gas. Thus, we have

$$n(z)\sigma(z) = \int_{L_{min}}^{\infty} \Phi(L) \cdot f_c \pi R^2(L) dL, \quad (9.36)$$

where $\sigma(z) = \pi R^2$, and where $R = R(L)$ is assumed to scale with galaxy luminosity. The term f_c is the covering fraction of absorbing gas for W_{min} , and L_{min} is the lower limit to the luminosity function of galaxies that actually contribute to the population of absorbers. The luminosity function is described by a Schechter function

$$\Phi(L) = \Phi^* \left(\frac{L}{L^*} \right)^{-\alpha} \exp \left(-\frac{L}{L^*} \right), \quad (9.37)$$

where α is the power index of the faint-end slope, L^* is the characteristic luminosity, and Φ^* is the number density of galaxies having $L = L^*$. The absorbing cross section is assumed to scale with galaxy luminosity, though this assumption can be relaxed. Invoking a Holmberg-like relation, we have

$$R(L) = R_* \left(\frac{L}{L^*} \right)^\beta, \quad (9.38)$$

where β is the power index for the luminosity scaling, and R_* is the projected radial extent the absorbing gas associated with an L^* galaxy.

Having measured $\mathcal{N}(z)$ and using the above assumed luminosity relationships, we wish to determine R_* . Setting $t = L/L^*$, and substituting Eqs. 9.37 and 9.38 into Eq. 9.36, we have

$$n(z)\sigma(z) = \pi f_c \Phi^* R_*^2 \int_{L_{min}}^{\infty} t^{2\beta-\alpha} e^{-t} dt. \quad (9.39)$$

The integral of Eq. 9.39 is proportional to the the Incomplete Γ function, $Q(a, b) = \Gamma(a, b)/\Gamma(a)$, where

$$\Gamma(a, b) = \int_b^{\infty} x^{a-1} e^{-x} dx, \quad (9.40)$$

with the condition $a > 0$, and where the Γ function is given by

$$\Gamma(a) = \int_0^{\infty} x^{a-1} e^{-x} dx. \quad (9.41)$$

The properties of the Incomplete Γ function are that $\Gamma(a, 0) = \Gamma(a)$, which applies in the case $L_{min} = 0$. Examination of Eqs. 9.39 and 9.40 yields $a = 2\beta - \alpha + 1$. The evaluation of $\Gamma(a, b)$ and $\Gamma(a)$ can be found in look-up tables or can be determined numerically (see *Numerical Recipes*, pp 206–210). We can thus rewrite Eq. 9.39 in terms of Γ ,

$$n(z)\sigma(z) = \pi f_c \Phi^* R_*^2 \Gamma(2\beta - \alpha + 1, L_{min}). \quad (9.42)$$

Finally, substituting Eq. 9.42 into Eq. 9.19 and rearranging for R_* , we have the radial extent of absorbers associated with an L_* galaxy

$$R_* = \left[\frac{c}{H_o} \frac{\pi f_c \Phi^*}{\mathcal{N}(z)} \frac{dX}{dz} \cdot \Gamma(2\beta - \alpha + 1, L_{min}) \right]^{-1/2}, \quad (9.43)$$

where the expression is evaluated for $z = \langle z \rangle$ of the redshift range over which absorbers are observed, $\mathcal{N}(z)$ is the measured redshift number density, and where dX/dz is given by Eq. 2.177 for

$$\frac{dX}{dz} = \frac{(1+z)^{2+\varepsilon}}{\sqrt{\Omega_m(1+z)^3 + \Omega_\Lambda}},$$

where ε has been determined from the data. For the Friedmann cosmology, Eq. 2.179 is used, giving

$$\frac{dX}{dz} = (1+z)^\gamma,$$

where γ has been determined from the data.

To obtain R_* in units of kiloparsecs, a useful and simplified form of Eq. 9.43 is

$$R_* \simeq 100 \left[\frac{f_c \Phi_{-2}^*}{\mathcal{N}(z)} \frac{dX}{dz} \cdot \Gamma(2\beta - \alpha + 1, L_{min}) \right]^{-1/2} h^{-1} \text{kpc}, \quad (9.44)$$

where Φ_{-2}^* is unitless and defined by $\Phi^* = \Phi_{-2}^* \times 10^{-2} \text{ Mpc}^{-3}$. Typical values of Φ_{-2}^* range between 1–4 for normal bright galaxies and 7–9 for low surface brightness galaxies.

Commonly, the covering factor is taken as $f_c = 1$. However, the covering factor “correction” of R_* can be generalized to account for other corrections. For example, not all galaxies may have extended gaseous envelopes and so not be associated with absorbers. This can be thought as a fractional correction, f_{abs} . The above formalism assumes spherical geometry of the absorber cross section. If the absorbers are flattened, then a geometric correction term, f_{geo} , would apply to the cross section. Therefore, the covering factor can be thought of as the product of several factors

$$f_c = f_{abs} f_{cov} f_{geo}, \quad (9.45)$$

where f_{abs} is the fraction of galaxies that give rise to absorbers, f_{cov} is the actual covering factor of the gas in the sky-projected geometric cross section of the absorber, and f_{geo} accounts for the sky-projected geometrical departure from a sphere. If the absorbers are spherical $f_{geo} = 1$, and if they are thin disks then $f_{geo} = 0.5$ (accounting for the random distribution of disks projected onto the sky).

There is a complex mathematical relationship between the parameters, α , β , and L_{min} that governs size estimates for absorbers. However, there are clear physical interpretations how each of these parameters govern R_* . In Figure 9.4, the component parts of the product $n(z)\sigma(z)$ are illustrated for selected parameter values.

The luminosity function, $\Phi(L)$, is shown in Figure 9.4 (upper left), for three values of the faint-end slope, α . Note that all curves are normalized at $L = L^*$. The ratio R/R_* is shown in Figure 9.4 (upper right) for two gas cross section dependencies, β . The product of $\Phi(L)R^2(L)$ provides the functional form of the integrand of the Γ function in Eq. 9.43. As shown in the lower left panel Figure 9.4, the larger β value suppresses the faint-end

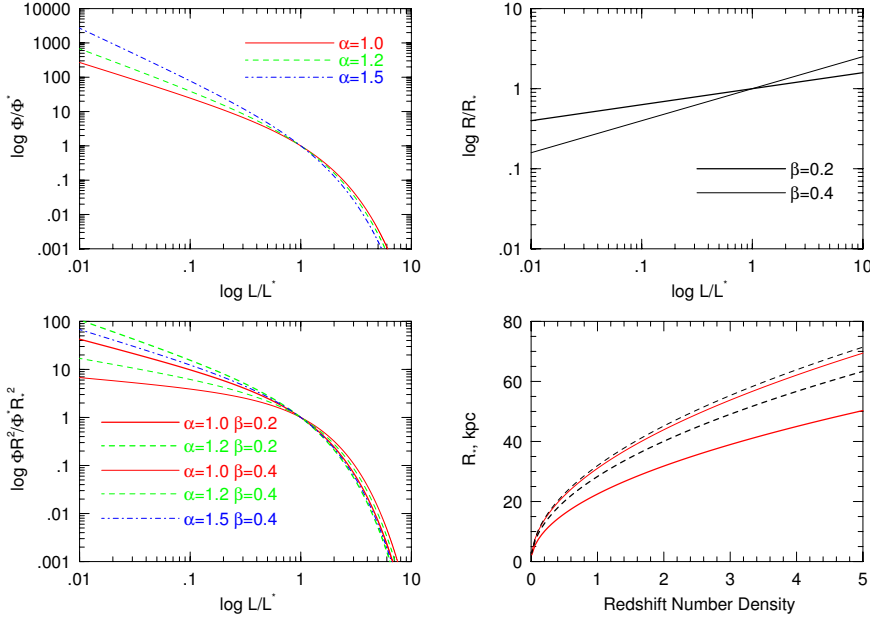


Figure 9.4: — (upper left) The luminosity function for three faint-end slopes, α , as a function of L/L_* . — (upper right) The dependence of the gas cross section for two β values. — (lower left) The integrand of the Γ function, the product of the luminosity function and the luminosity weighted gas cross section. The color coded legend gives the α - β combinations. — (lower right) R_* as a function of $\mathcal{N}(z)$ for $\alpha = 1.0$ with $\beta = 0.2$ (thick solid curve) and $\beta = 0.4$ (thin solid curve). The dependence of R_* on L_{min} is shown with the dashed curves for each α - β combination.

slope, reducing the cross-sectional contribution of the lowest luminosity galaxies. Note that the bright end is also elevated compared to $\Phi(L)$.

Note that the faint end dominates the number of contributing galaxy halos. Cutting the integral at a given L_{min} cuts off fewer (more) contributing galaxies to the redshift path density of absorbers for a flatter (steeper) faint-end slope. Thus, for the steeper faint-end slope, larger halos sizes are required of $L > L_{min}$ galaxies to hold $n(z)\sigma(z)$ constant at its observationally constrained value. As such, a smaller β results in a more sensitive behavior of R_* as a function of L_{min} .

Figure 9.4 (lower right) shows R_* as a function of $\mathcal{N}(z)$ for $L_{min} = 0$ and $\alpha = 1.0$ with $\beta = 0.2$ (thick solid curve) and $\beta = 0.4$ (thin solid curves). The normalization is for $\Phi_{-2}^* = 3.0$, $f_c = 1$, and an $\varepsilon = 0$ evolution parameter for the currently fashionable concordance cosmological model. The dashed lines are for $L_{min}/L_* = 0.05$ for $\beta = 0.2$ (thick dashed curve) and $\beta = 0.4$

(thin dashed curve). Note the greater sensitivity to L_{min} for the smaller value of β , which does not substantially flatten the faint-end slope of the product $\Phi(L)R^2(L)$.

9.5 Equivalent Width Distribution

The equivalent width distribution, EWD, is defined to give the number of systems per unit redshift with equivalent width, W , per unit equivalent width. Thus, the distribution function is normalized to the observed redshift density, $\mathcal{N}(z)$,

$$\int_{W_{min}}^{\infty} n(W) dW = \mathcal{N}(z). \quad (9.46)$$

Observationally, the EWD of different classes of absorbers has been well described by an exponential function,

$$n(W) dW = \frac{N_*}{W_*} \exp\left(-\frac{W}{W_*}\right) dW, \quad (9.47)$$

or by a power-law function

$$n(W) dW = C W^{-\beta} dW. \quad (9.48)$$

However, when a large dataset is available, redshift evolution in the EWD can be parameterized. Consider the exponential form of the EWD. The normalization, N_* , and characteristic equivalent width, W_* , may evolve with redshift according to

$$N_*(z) = N_*(1+z)^\epsilon \quad \text{and} \quad W_*(z) = W_*(1+z)^\delta. \quad (9.49)$$

Then, the redshift EWD for the exponential function is written,

$$\frac{d^2 n(W, z)}{dW dz} = \frac{N_*(z)}{W_*(z)} \exp\left[-\frac{W}{W_*(z)}\right], \quad (9.50)$$

is written

$$\frac{d^2 n(W, z)}{dW dz} = \frac{N_*}{W_*} (1+z)^{\epsilon-\delta} \exp\left[-\frac{W}{W_*} (1+z)^{-\delta}\right]. \quad (9.51)$$

For the power-law EWD, we have

$$\frac{d^2 n(W, z)}{dW dz} = C (1+z)^\epsilon W^{-\beta_* (1+z)^\delta}, \quad (9.52)$$

assuming

$$C(z) = C(1+z)^\epsilon \quad \text{and} \quad \beta(z) = \beta_*(1+z)^\delta. \quad (9.53)$$

The values of ϵ , δ , and W_* (exponential) or β (power law) can be determined from the maximum likelihood method (§ 3.5), following which the normalization, N_* or C , is determined from

$$N_{abs} = \int_{z_{min}}^{z_{max}} \int_{W_{min}}^{\infty} \frac{d^2 n(W, z)}{dW dz} g(W, z) dW dz, \quad (9.54)$$

where N_{abs} the number of absorption systems with $W \geq W_{min}$ detected in the survey.

9.6 Two-Point Velocity Clustering

In low resolution spectra of $1000 \leq R \leq 3000$, the velocity resolution is $300 \geq \Delta v \geq 100 \text{ km s}^{-1}$, which follows from $v/c = \Delta\lambda/\lambda = 1/R$. Thus, provided the spectra cover a large observed wavelength range, they can be used to quantify the large scale velocity clustering of absorbers. Higher resolution spectra are required to examine the clustering on the velocity scales internal to galaxy halos. We address this in Chapter 8.2.

The two-point velocity clustering function (TPCF) is analogous to the two-point clustering function for galaxies. The differential probability of finding a pair of absorbers with co-moving velocity splitting $\Delta v \rightarrow \Delta v + d\Delta v$ is written,

$$dP = \Phi_o [1 + \xi(\Delta v)] d\Delta v \quad (9.55)$$

where Φ_o is the number density of absorbers per co-moving velocity, and $\xi(\Delta v)$ is the correlation amplitude,

$$\xi(\Delta v) = \frac{N_p(\Delta v)}{N'_p(\Delta v)} - 1, \quad (9.56)$$

where $N_p(\Delta v)$ is the observed number of pairs with velocity separation Δv and $N'_p(\Delta v)$ is the estimated number of pairs with velocity separation Δv assuming they are randomly distributed in redshift. A statistically significant measurement of clustering occurs when $\xi(\Delta v)$ is inconsistent with zero.

Computing $N_p(\Delta v)$ directly from the data is straight forward. Estimating $N'_p(\Delta v)$ is critical and must account for both the finite range of the spectra and the detection sensitivity as a function of Δv . Analogous to the redshift path sensitivity function is the velocity splitting sensitivity function, $G(\Delta v)$, which yields the relative probability of detecting a velocity

splitting of Δv from each observed absorbing system,

$$G(\Delta v) = \sum_{j=1}^{N_{abs}} \int_{z_1}^{z_2} g_i(W_{min}, z) dz, \quad (9.57)$$

where the sum is taken over all absorbers and the index i for $g(W_{min}, z)$ references the quasar i in which system j is found. The integral is over the redshift window

$$z_1 = z_j - \Delta z(\Delta v) \quad \text{and} \quad z_2 = z_j + \Delta z(\Delta v), \quad (9.58)$$

corresponding to the velocity separation Δv , following,

$$\Delta z(\Delta v) = \frac{\Delta v}{c} (1 + z_j), \quad (9.59)$$

where z_j is the redshift of absorber j . In practice, the integral in Eq. 9.57 can be computed as a sum over the (W_{min}, z) grid in the z direction, yielding

$$\Delta Z_{ij}(\Delta v) = \int_{z_1}^{z_2} g_i(W_{min}, z) dz = \sum g_i(W_{min}, z) \delta z, \quad (9.60)$$

for $z_1 \leq z \leq z_2$ on the grid, where δz is the bin size of the grid in the redshift direction (see § 9.2). Each $\Delta Z_{ij}(\Delta v)$ is the redshift path over which an absorbers with $W \geq W_{min}$ could be detected within velocity splitting Δv of absorber j in quasar i (the quasar in which absorber j resides). Thus, we have

$$G(\Delta v) = \sum_{j=1}^{N_{abs}} \Delta Z_{ij}(\Delta v), \quad (9.61)$$

which follows from Eqs. 9.11 and 9.12. Eq. 9.61 provides a more straight forward interpretation of Eq. 9.57. The function $G(\Delta v)$ is the total redshift path over which absorbers with $W \geq W_{min}$ could be detected within velocity splitting Δv . The estimate of $N'_p(\Delta v)$ is obtained by normalizing the integral of $G(\Delta v)$ to $N_p(\Delta v)$, the number of observed absorbers with velocity splitting Δv ,

$$N_p(\Delta v) = K \int_0^{\Delta v} G(\Delta v) d\Delta v., \quad (9.62)$$

giving

$$N'_p(\Delta v) = K \cdot G(\Delta v). \quad (9.63)$$

Thus, correlation amplitude is

$$\xi(\Delta v) = \frac{N'_p(\Delta v)}{K \cdot G(\Delta v)} - 1. \quad (9.64)$$

9.7 Mean Gas Density

The gas density of a class of absorber at a given redshift is defined in terms of the critical density,

$$\Omega_g(z) = \frac{\langle \rho(z) \rangle}{\rho_c}, \quad (9.65)$$

where $\langle \rho(z) \rangle$ is the mean mass density at z and ρ_c is the critical density.

When the gas is ionized, we will show that ionization corrections are required. If we survey metal lines, such as the Mg II, C IV, or O VI doublets, both ionization corrections and metallicities are required to estimate $\Omega_g(z)$.

9.7.1 Neutral Hydrogen Systems

The ionization fraction of H I is negligible for DLAs, and thus no ionization correction is required. Consider neutral H I absorbers with mean neutral hydrogen column density $\langle N_H \rangle$.

The mean mass density per absorber in a proper reference frame is

$$\langle \rho \rangle = \mu m_H \langle n \rangle, \quad (9.66)$$

where m_H is the mass of the hydrogen atom, $\langle n \rangle$ is the mean number density of atoms per absorber, and $\mu = 1/(1 - Y) = 1.33$ is the mean “molecular” weight to account for the contribution of helium by mass, $Y = 0.25$, assuming all metals are an insignificant contribution to the mass density. The cumulative mean number density of atoms in a redshift interval is the product of the mean hydrogen column density per absorber, $\langle N_H \rangle$, and the redshift density of absorbers, $\mathcal{N}(z)$, intercepted in the interval $l \rightarrow l + dl$,

$$\langle n \rangle = \langle N_H \rangle \mathcal{N}(z) \frac{dz}{dl}, \quad (9.67)$$

where the redshift density, $\mathcal{N}(z)$, is given by Eq. 9.19, and $dz/dl = (dl/dz)^{-1}$ is the inverse of Eq. 9.71. The mean proper mass density is then written,

$$\langle \rho \rangle = \mu m_H \langle N_H \rangle \mathcal{N}(z) \frac{dz}{dl}. \quad (9.68)$$

The proper mass density decreases with the volume expansion of the universe according to $\rho(z) = \rho/(1 + z)^3$, giving the co-moving mean mass density at redshift z for a non-evolving population of absorbers

$$\langle \rho(z) \rangle = \mu m_H \frac{\langle N_H \rangle \mathcal{N}(z)}{(1 + z)^3} \frac{dz}{dl}. \quad (9.69)$$

In terms of the critical mass density of the universe, we have

$$\Omega_g(z) = \frac{\langle \rho(z) \rangle}{\rho_c} = \frac{\mu m_H}{\rho_c} \frac{\langle N_H \rangle \mathcal{N}(z)}{(1+z)^3} \frac{dz}{dl}, \quad (9.70)$$

where (Eq. 9.71),

$$\frac{dl}{dz} = \frac{c}{H_o} \frac{1}{(1+z)E(z)}, \quad (9.71)$$

and where c/H_o is the Hubble distance, and $E(z)$ is given by Eq. 2.80. Substituting $dz/dl = (dl/dz)^{-1}$ into Eq. 9.70, gives

$$\Omega_g(z) = \frac{H_o}{c} \frac{\mu m_H}{\rho_c} \frac{E(z)}{(1+z)^2} \langle N_H \rangle \mathcal{N}(z). \quad (9.72)$$

For a Friedmann cosmology, $\Omega_\Lambda = 0$, Eq. 9.71 is written

$$\frac{dl}{dz} = \frac{c}{H_o} \frac{1}{(1+z)^2 \sqrt{1+2q_o z}}, \quad (9.73)$$

where $E(z)$ is given by Eq. 2.83. Substitution into Eq. 9.70, gives

$$\Omega_g(z) = \frac{H_o}{c} \frac{\mu m_H}{\rho_c} \frac{\sqrt{1+2q_o z}}{(1+z)} \langle N_H \rangle \mathcal{N}(z). \quad (9.74)$$

Since the gas density at any given redshift is dependent upon local processes of star–gas cycles, and these processes are not causally connected to cosmological expansion, cosmological evolution in the gas density cannot be easily parameterized. It is common convention to write Ω_g in terms of the absorption distance $X(z)$, which yields a constant value for a non–evolving quantity. From Eq. 9.27 and the definition (Eq. 2.177) of dX/dz , we have

$$\mathcal{N}(z) = \mathcal{N}(X) \frac{dX}{dz} = \mathcal{N}(X) \frac{(1+z)^2}{E(z)}. \quad (9.75)$$

where $X(z)$ is given by Eq. 2.178. Substitution into Eq. 9.72 yields,

$$\Omega_g(X) = \frac{H_o}{c} \frac{\mu m_H}{\rho_c} \langle N_H \rangle \mathcal{N}(X), \quad (9.76)$$

where $X(z)$ is given by Eq. 2.178 and $\mathcal{N}(X)$ is given by Eq. 9.29. Since $\mathcal{N}(X) = (c/H_o)n(X)\sigma(X)$, we see that a statistically significant departure of $\Omega_g(X)$ from a constant is linked to evolution in the product $n(X)\sigma(X)$. Since Eq. 9.76 is independent of cosmology, the same relation results for a Friedmann cosmology, except that $X(z)$ is given by Eq. 2.180.

9.7.2 Metal Line Systems

Since $\langle N_{\text{H}} \rangle$ is the mean hydrogen column density per absorber, then Eq. 9.76 estimates the mean gas mass. However, the mean density of a particular ionization species (i.e., Mg II, C IV, O VI, or H I) can be obtained similarly to Eq. 9.76 using

$$\Omega_{xj} = \frac{H_o}{c} \frac{m_x}{\rho_c} \langle N(x^j) \rangle \mathcal{N}(X), \quad (9.77)$$

where $\langle N(x^j) \rangle$ is mean column density per absorber for chemical species x (i.e., carbon, oxygen) in ionization stage j (i.e., C^{+3} for C IV, O^{+5} for O VI), and m_x is the mass of species x .

To obtain the mean gas density of absorbers selected by metal lines, both ionization correction and metallicity correction must be applied to Eq. 9.77. For example, C IV traces the third ionization stage of carbon, C^{+3} . Thus, the total carbon column density is not measured, but only a fraction of the total depending upon the ionization balance in the gas. Furthermore, the abundance of carbon in solar metallicity gas is roughly 1 part in 3400, or $\sim 3 \times 10^{-4}$. In absorption line systems, this abundance can be an additional factor of 30 to 300 smaller.

Adding these two “corrections” to Eq. 9.77, we have

$$\Omega_g = \frac{\mu m_{\text{H}}}{m_x} \frac{\Omega_{xj}}{\langle f(x^j)(x/\text{H}) \rangle} = \frac{H_o}{c} \frac{\mu m_{\text{H}}}{\rho_c} \frac{\langle N(x^j) \rangle \mathcal{N}(X)}{\langle f(x^j)(x/\text{H}) \rangle}, \quad (9.78)$$

The ionization fraction, $f(x^j)$, is the ratio of the number density of chemical species x in ionization stage j to the total number density of species x ,

$$f(x^j) = \frac{n(x^j)}{n(x)}, \quad (9.79)$$

where

$$n(x) = \sum_{i=1}^{M_x} n(x^i), \quad (9.80)$$

and where M_x is the number of ionization stages for species x . The ionization fractions must be obtained through photoionization or collisional ionization models (see § 11).

The term (x/H) is the abundance ratio of species x relative to the total hydrogen in the absorbing cloud. Note that the quantity

$$\langle f(x^j)(x/\text{H}) \rangle = \frac{1}{m} \sum_{i=1}^m f_i(x^j)(x/\text{H})_i \quad (9.81)$$

is the mean over all absorbers, m , since not all systems will have identical ionization and chemical conditions. One method to approximate Eq. 9.81 is

$$\langle f(x^j)(x/H) \rangle \approx \frac{\mu m_H}{m_x} \frac{\Omega_{x^j}}{\Omega_b} f_g, \quad (9.82)$$

where $\Omega_b h^2 = 0.02$ is the cosmic baryon density, and f_g is the fraction of the baryonic mass in gas. The value of f_g will depend upon the type of gas being probed; in cold collapsed structures $f_g \sim 1$, but in more diffuse structures, $f_g \sim \Omega_b/\Omega_m = 0.02/0.3 = 0.067$.

In cases where the neutral hydrogen column density, N_{HI} , is also measured, a second method to approximate Eq. 9.81 is ionization modeling. Assuming either photoionization or collisional ionization equilibrium, the metallicity of the i th absorber in the sample is

$$(x/H)_i = \frac{N_i(x)}{N_{\text{H},i}} = \frac{N_i(x^j)}{f_i(x^j)} \frac{f_{\text{HI},i}}{N_{\text{HI},i}}, \quad (9.83)$$

which after substituting into Eq. 9.81, yields

$$\langle f(x^j)(x/H) \rangle = \frac{1}{m} \sum_{i=1}^m \frac{f_{\text{HI},i}}{N_{\text{HI},i}} N_i(x^j), \quad (9.84)$$

where the $N_i(x^j)$ are the measured column densities of chemical species x in ionization state j , and the $f_{\text{HI},i} = N_{\text{HI},i}/N_{\text{H},i}$ are the ionization corrections for hydrogen obtained from the models.

Under the highly simplifying assumption that all systems of a given class have roughly identical ionization conditions, then Eq. 9.84 simplifies to

$$\langle f(x^j)(x/H) \rangle \approx \left\langle \frac{f_{\text{HI}}}{N_{\text{HI}}} \right\rangle \langle N_i(x^j) \rangle = \langle N_{\text{H}} \rangle \langle N_i(x^j) \rangle, \quad (9.85)$$

from which Eq. 9.76 is recovered from Eq. 9.78.

9.7.3 Obtaining $\langle N \rangle \mathcal{N}(X)$

To empirically estimate Ω_g , both the mean column density per absorber, $\langle N \rangle$, and the absorption distance density of absorbers are required. The latter is measured directly from the survey using the formalism in Eqs. 9.33 and 9.29. There are two common methods for estimating $\langle N \rangle$:

1. Commonly, a distribution function, often a power law, is assumed and evaluate. The parameters of the distribution function are determined directly from the data. The drawback is that, to obtain $\langle N \rangle$, the

required integration will be from some N_{min} of the survey to $N_{max} = \infty$. Thus, an N_{max} from the largest column density in the observed sample is often used. As we will show, the computed value of Ω_g will be most sensitive to N_{max} , which is troublesome for small samples.

2. The mean value of column density can be determined by taking the average of the measured column densities in the survey. Again, the solution is most sensitive to the largest column densities in the observed sample.

Both of these techniques are outlined below.

9.7.4 Column Density Distribution

The mean column density per absorption distance can be found from the first moment of the column density distribution function, $f(N)$, which is defined to be the mean number of absorbers per unit column density per unit absorption distance. By definition,

$$\int_{N_{min}}^{\infty} f(N) dN = \mathcal{N}(X), \quad (9.86)$$

for which the expectation value of N is

$$\langle N \rangle \mathcal{N}(X) = \int_{N_{min}}^{\infty} N f(N) dN. \quad (9.87)$$

Based upon observations, the data suggest a power-law form where

$$f(N) = C N^{-\beta}, \quad (9.88)$$

where C is the normalization constant, and β is the power-law slope, and the normalization is given by Eq. 9.86. Note that we have the condition $\beta \neq 2$. The values of C and β and their uncertainties are determined directly by fitting the data to Eqs. 9.86 and 9.88 using the maximum likelihood method. Integrating, we have

$$\langle N \rangle \mathcal{N}(X) = C \int_{N_{min}}^{N_{max}} N^{1-\beta} dN = \frac{C}{2-\beta} \left(N_{max}^{2-\beta} - N_{min}^{2-\beta} \right), \quad (9.89)$$

where we have replaced the upper limit of the integral with N_{max} , often taken to be the maximum column density in the observed sample. Substitution into Eq 9.76 for $\langle N \rangle \mathcal{N}(X)$, gives

$$\Omega_g(X) = \frac{H_o}{c} \frac{\mu m_H}{\rho_c} \frac{C}{2-\beta} \left(N_{max}^{2-\beta} - N_{min}^{2-\beta} \right), \quad (9.90)$$

with uncertainty

$$\sigma_{\Omega_g} = \Omega_g \left[\left(\frac{\sigma_C}{C} \right)^2 + \sigma_\beta^2 \left(R + \frac{1}{(2-\beta)} \right)^2 \right]^{1/2}, \quad (9.91)$$

where

$$R = \frac{N_{max}^{2-\beta} \ln(N_{max}) - N_{min}^{2-\beta} \ln(N_{min})}{N_{max}^{2-\beta} - N_{min}^{2-\beta}} \simeq \ln(N_{max}), \quad (9.92)$$

and where σ_C and σ_β are the uncertainties determined for C and β , respectively. Note that $R \simeq \ln(N_{max})$ applies when $N_{max} \gg N_{min}$.

Note that Ω_g is most sensitive to N_{max} , not N_{min} . This is good news in that high sensitivity surveys are not required to estimate Ω_g , but bad news in that the sample size needs to be very large to reduce the Poisson noise at large N .

9.7.5 Mean Column Density

In a survey, the mean column density of observed systems is

$$\langle N \rangle = \frac{1}{m} \sum_{i=1}^m N_i \quad \text{for } N_i \geq N_{min}, \quad (9.93)$$

where N_{min} is the minimum detectable column density, and m is the number of observed absorption systems with $N > N_{min}$. From $\mathcal{N}(X) = m/\Delta X$, the number of systems in the absorption distance ΔX is written

$$m = \mathcal{N}(X) \Delta X, \quad (9.94)$$

where ΔX is given by Eq. 9.33. Equating Eq. 9.87 and Eq. 9.93, we find

$$\langle N \rangle \mathcal{N}(X) = \int_{N_{min}}^{\infty} N f(N) dN = \frac{1}{\Delta X} \sum_{i=1}^m N_i \quad (9.95)$$

where the uncertainty is given by

$$\sigma_{\langle N \rangle \mathcal{N}(X)} = \frac{1}{\Delta X} \left[\frac{m}{m-1} \sum_{i=1}^m (N_i - \langle N \rangle)^2 \right]^{1/2}. \quad (9.96)$$

Substituting Eq. 9.95 into Eq. 9.95, the resulting expression for the gas density is

$$\Omega_g(X) = \frac{H_o}{c} \frac{\mu m_H}{\rho_c} \frac{1}{\Delta X} \sum_{i=1}^m N_i \quad (9.97)$$

with uncertainty

$$\sigma_{\Omega_g} = \frac{H_o}{c} \frac{\mu m_{\text{H}}}{\rho_c} \sigma_{\langle N \rangle \mathcal{N}(X)}. \quad (9.98)$$

As with the distribution function approach, Ω_g is sensitive to the largest column density in the sample.

